



AN ELECTRON FRACTOGRAPHIC STUDY OF  
THE INFLUENCE OF ANNEALING CONDITIONS  
UPON DUCTILE RUPTURE PROCESS IN Cu-Zn BRASSES

TAHA GOMAA<sup>\*</sup>, NABIL FAT-HALLA<sup>\*\*</sup>, MAZEN NEGM<sup>\*\*</sup> AND  
MOHAMMAD REFAI<sup>\*\*</sup>

ABSTRACT

An investigation on the fracture phenomena of ( $\alpha+\beta$ ) brass, polycrystalline alloys, has been conducted using the scanning electron microscope (S.E.M.). The as-rolled alloys (starting material) were subjected to different conditions of annealing. Then, tensile tests were carried out at room temperature on three categories of specimens being; (i) as-rolled, (ii) annealed at 923K for 86.4ks, and (iii) annealed at 873K for 2 Ms plus 1.4 Ms at 800K. All types of specimens showed ductile fracture. Fracture surfaces were then observed by the S.E.M. on both the macro-and microscopic scales. All specimens exhibited a transgranular mode of fracture. Fracture surfaces revealed some changes in the pattern observed on each phase due to annealing conditions. Dimple pattern was observed on the  $\beta$ -phase, although different dimple size existed for different types of specimens. On the other hand, on the  $\alpha$ -phase, fracture surface, smooth ripple pattern was observed, additionally, large dimples were detected on the  $\alpha$ -surface. In essence, the present results not only confirmed previous results on single-and bi-crystals of brass but also throw the light on more details about the fracture phenomena of brass which was not reported before.

INTRODUCTION

The large depth of field, and high useful magnification available in the scanning electron microscope (S.E.M.) make this instrument an admirable tool in the study of fracture topographies. Electron fractography of micromechanisms of fracturing processes, macro-and micro-features of the fracture surface, might lead to information which will aid in the design of stronger tougher alloys.

Ductile fracture of commercial metals and alloys involves two basic modes, the fibrous mode and the shear mode [1]. Fibrous fracture leads to a fracture surface covered with equiaxed dimples [2]. The shear mode of ductile fracture leads to fracture surfaces covered with strongly - oriented parabolic dimples [1] : Previous work [3] has shown that sheet

\* Graduate school, Mechanical Department, Faculty of Engineering,  
AL Azhar University.

\*\*Mechanical Department, Faculty of Engineering, AL Azhar University.

tensile specimens of brasses fracture entirely by the shear mode [4].

A number of studies have been made on the problem of nucleation of voids in the absence of inclusions which suggest that cracks could form at grain boundaries due to dislocation pile-up [4] or by coalescence of vacancies produced by moving dislocations [5]. Also, crack propagation in single crystals of high purity has shown to develop by coalescence of crystallographic holes in the reoriented material formed in the necked region [6].

Recently some investigators studied the fracture of  $\alpha$ -brass and  $\beta$ -brass single crystals [7]. The fracture phenomena of ( $\alpha/\beta$ ) brass bicrystals have been recently reported [7-12]. However there is a lack of information in the literature about the fracture phenomena of ( $\alpha+\beta$ ) brass polycrystalline alloys. Although some researches [13-17] studied the fracture of this alloy however these researches have not taken into consideration the micro-features inside the fracture surface.

Therefore, in the present investigation a S.E.M. was used to examine both macro-and micro-features of the fracture phenomena of the ( $\alpha+\beta$ ) brass two phase polycrystalline alloy. The change in the fracture pattern due to change of the annealing conditions are to be presented and discussed. In general, a better understanding of the effect of grain-and phase-boundaries on the fracture phenomena is shown for the ( $\alpha+\beta$ ) brass polycrystalline alloy.

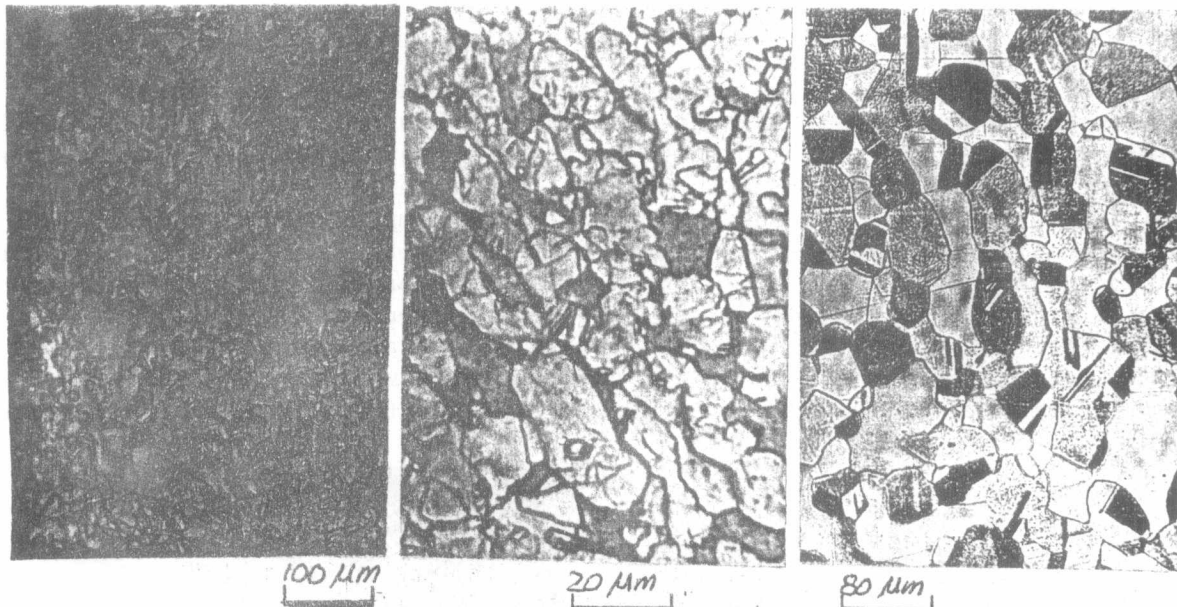
#### EXPERIMENTAL PROCEDURE

( $\alpha+\beta$ ) brass alloy was received from Helwan Co. for Non-Ferrous Industries on the form of hot extruded plates 12 mm thickness of about 40 wt % Zn content. The plate thickness have been reduced to 5 mm by successive rolling processes at room temperature each of which was followed by an intermediate annealing process for 3.6 ks at 873K, then cooled in open air. Sheets were then chemically cleaned and washed by hot water at 353K, followed by cold water washing and then dried. Tensile specimens were machined to the gauge dimensions 28x7x5 mm<sup>3</sup>. Specimens were subjected to two stage annealing being; at 873K for 2 Ms and followed by annealing at 800 K for 1.4 Ms. Tensile tests were conducted on M.T.S. machine at room temperature at a strain rate of  $7 \times 10^{-2} \text{ s}^{-1}$  up to fracture. The S.E.M. used in the present investigation was of the type (Cambridge Steroscan 600).

#### RESULTS

The microstructure of the ( $\alpha+\beta$ ) brass duplex alloy which was received as-extruded is shown in Fig.1(a). Homogeneous distribution of  $\alpha$ -grains in a  $\beta$ -matrix can be observed. After the room temperature rolling mentioned in the procedure, the microstructure showed some elongation in the grains (Cf. Fig.1(b)). After the step annealing, mentioned previously, the microstructure as can be seen in Fig.1(c), exhibited large equiaxed  $\alpha$ -grains in a  $\alpha$ -matrix, additionally, more or less straight grain-and interphase-boundaries are observed.

The  $\alpha$ -grain size increased from 15  $\mu\text{m}$  in case of extruded specimens to 80  $\mu\text{m}$  after prolonged annealing as estimated by the line interception method. As can be observed in Fig.1(c), three types of boundaries do exist being the  $\alpha/\alpha$ ,  $\alpha/\beta$  and  $\beta/\beta$ , while the later can not be



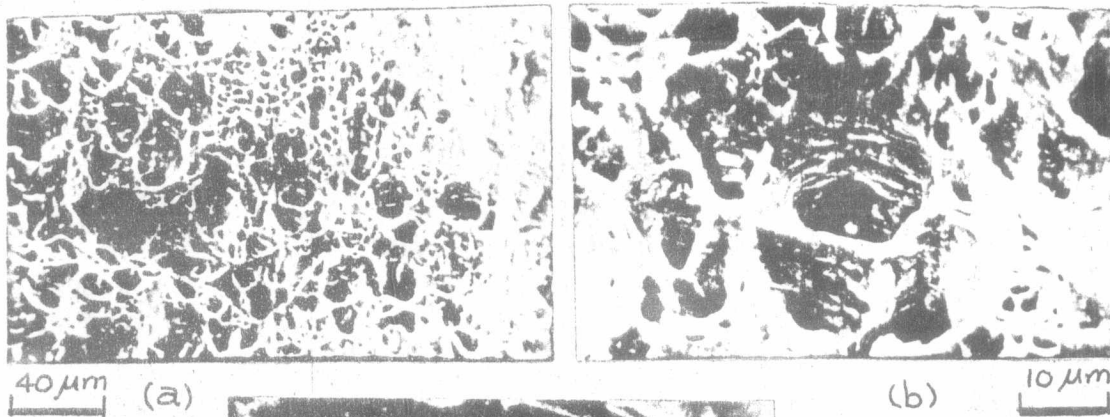
(a)

(b)

(c)

Fig.1. Shows the microstructure; (a) as extruded, (b) as rolled, and (c) after step annealing.

observed in Fig.1(a,b). Fig.1(a-c) shows the well known twinning phenomenon in the  $\alpha$ -grains. The fracture results will be presented as three categories being (i) as-rolled specimens, (ii) intermediate annealing specimens and (iii) full annealing specimens.

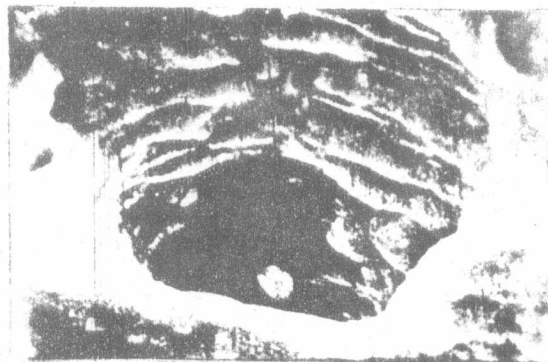


40 μm

(a)

(b)

10 μm



(c)

4 μm

Fig.2. Scanning electron micrography of a fracture surface produced in a tensile test on a sample specimen of group (i).

The rolled specimens showed more or less a cup and cone fracture on a macroscopic scale. The fracture surface as observed in Fig.2 for a sample specimen consists of large dimples on the  $\alpha$ -phase and small dimples on the  $\beta$ -phase. Fig.2(a) shows clearly that the fracture surface was covered by two dimple patterns of fracture, being; large dimples and small dimples. Additionally, an interesting result, of the present investigation, can also be observed through Fig.2(b). The central portion of Fig.2(b), observed on the  $\alpha$ -phase, showed deep dimple having inclusion at the apex of it. Additionally the upper side showed others having no inclusions. Moreover, it was clearly shown (Cf.Fig.2(c)) that the side walls of each of this type of dimples was covered by a smooth ripple pattern. These interesting results will be discussed later.

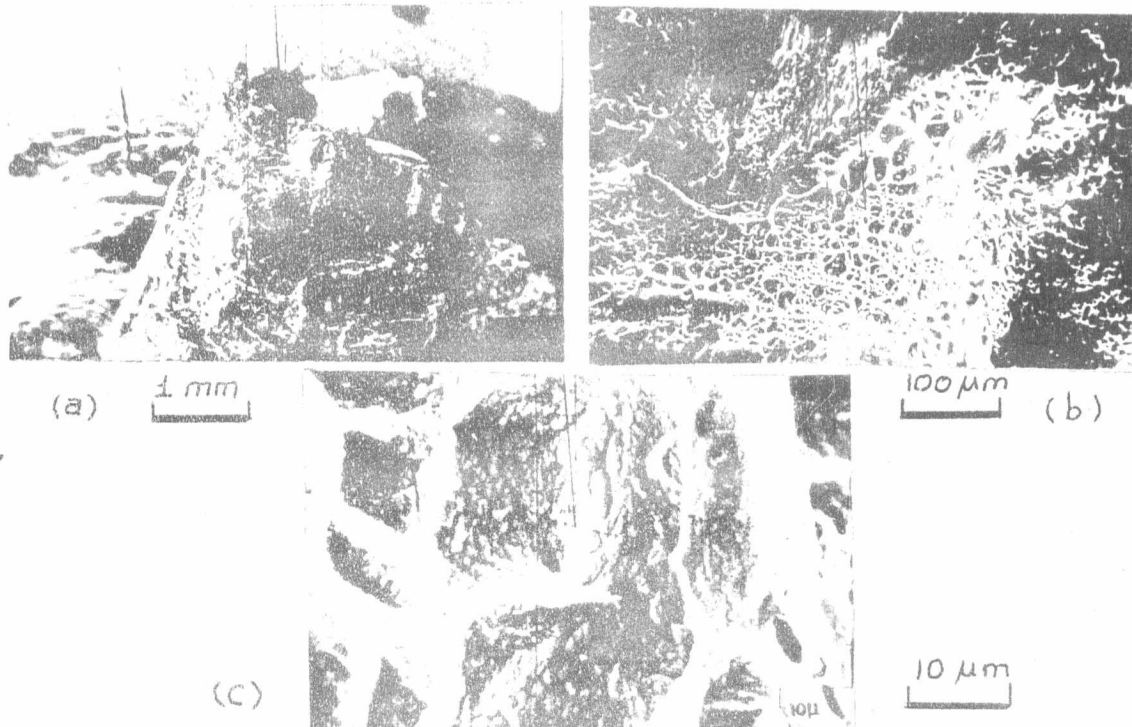


Fig.3 Scanning electron micrographs of a fracture surface of a sample specimen of group (ii), showing; (a) fracture type (b) surface general features, (c) ripple pattern of  $\alpha$ -grains.

The annealed specimens as in Fig.3(a) showed a type of Chisel fracture on a macroscopic scale. Fig.3(b) exhibits large dimples, small dimples and smooth areas in the upper left. Fig.3(c) is another example of the fracture pattern observed on the  $\alpha$ -phase which shows large dimples (although not deep as that observed in Fig.2(c)). It is clearly shown that the side walls of the dimples are covered with some sort of ripple pattern.

Fig.4(a) shows a slant fracture of the third group of full annealing specimens on a macroscopic scale. Fig.4(b) shows equiaxed shallow dimples and very smooth areas. Smooth ripple pattern was shown in Fig.4(c) at high magnification Fig.4(d) shows three patterns on the fracture surface being (i) very smooth ripple pattern (serpentine glide), left of photograph, smooth featureless pattern, in the middle, and large shallow dimples showed in the upper right of the photograph.



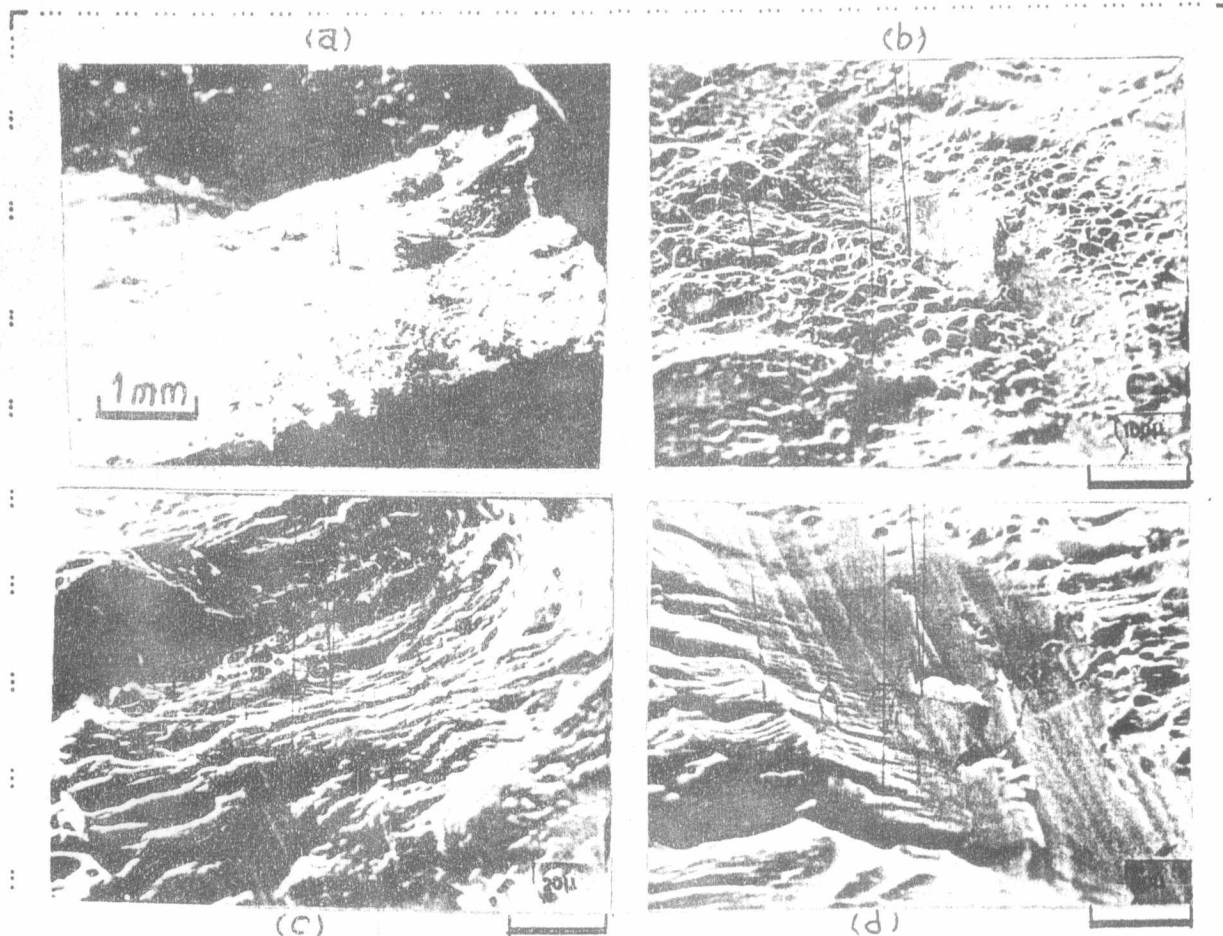


Fig.4. Scanning electron micrographs of fracture surface of a sample specimen of group (iii), showing; (a) macrophotograph of the fracture surface, (b) general surface features, (c) smooth ripple pattern of  $\alpha$ -grain, (d) smooth featureless pattern.

#### DISCUSSION

As shown from Fig.1(a-c) large equiaxed  $\alpha$ -grains were obtained having more or less straight interfaces, which was the main aim of the annealing process, which is in consistence with previous researches [18] as can be seen from Fig.1(c). The macro-fractography of the three groups showed different types of ductile fracture being, (i) cup and cone in the first group, (ii) Chisel in the second, and (iii) slant in the later. Change in these types occurred as direct result of change of grain size and change of the strength of components [19]. Fig.2(a-c) achieved Puttick & Cottroll conclusion [20] that the cavities in ductile fracture may be nucleated at inclusions and that foreign particles are a common nucleating site for cavities in ductile rupture, and also reinforced Roger's conclusion [20] that cavities may be nucleated in regions of very severe plastic flow without presence of inclusions as shown in Fig.2(a,b). Although  $\alpha$ - and  $\beta$ -phases exhibited dimple patterns for group (i) but  $\alpha$ -dimples are larger in comparison with  $\beta$ -dimples of the same specimen as shown in Fig.2(a,b) because  $\beta$ -phase component possesses higher strength than  $\alpha$ -phase component. By annealing the strength of the two phases decrease therefore the number of the nucleation sites decrease and that is why specimens of group (i) have small dimples in comparison with the other two groups as can be seen in Fig.3(b,c) and Fig.4(b). Additionally, the dimples became shallower in group (ii) and (iii) than those of (i) group for

the two-phase components due to the decrease of the triaxial stress.

Dimple pattern observed on the  $\alpha$ -phase either at inclusions or at localized severe deformation zones, the former can be reasonably assumed to be the same in the three groups (i.e. the inclusions content is assumed to be the same), thus we are interested in the second effect.  $\alpha$ -phase component observed in group (i) as small and deep dimples as can be seen from Fig. 2(a-c) that the  $\alpha$ -component exhibited a large number of small dimples because the nucleation sites number are believed to be high owing to the expected large number of localized severe deformation zones. As a result of the annealing process the strength of  $\alpha$ -component decrease due to the reasons mentioned before which leads to the presence of large shallow  $\alpha$ -dimples and the appearance of a new mode of fracture being a ripple pattern mode as shown in Fig.3(c) of group (ii). With full annealing,  $\alpha$ -phase exhibited ripple pattern and featureless zones due to the interaction between deformation bands or undeformed zones respectively with the fracture surface as can be seen in Fig.4(c) which exhibited the ripple pattern and Fig.4(d) which exhibited the featureless zones of group (iii). Some investigators have referred to those smooth features as having been formed by glide plane decohesion or by ductile cleavage [19].

$\beta$ -phase component exhibited small deep dimples in (i) group as can be seen from Fig.2(a). The dimples began to be larger and shallower in the other two groups as can be shown from Fig.3(b) and Fig.4(b) of group (ii) and (iii) respectively. By analogy to the discussion mentioned in the previous paragraph, the change in dimple size refer to the change of the number of nucleation sites (change of number of localized deformation zones). Additionally, the change from deep dimples into shallow dimples refer to the change of the strength of the  $\beta$ -component phase.

#### CONCLUSIONS

From the present research the following conclusions can be drawn.

1.  $\alpha$ -phase component exhibited dimple pattern in case of as rolled specimens, that pattern changed to a smooth ripple and featureless patterns by full annealing conditions. A mixed pattern of these two was observed for the intermediate annealing conditions specimens.
2.  $\beta$ -phase component exhibited dimple pattern for all cases but with several dimple sizes and depths due to the change of annealing conditions.

#### ACKNOWLEDGMENT

The present authors wishes to thank Dr. Eng. Abd Al Basset Al Sebai of Helwan Co. for the kind supply of the raw material. They also are indebted to Eng. M. Adel Beshir of the material testing laboratory of the National Research Center for the Chemical analysis.

#### REFERENCES

1. Beachem, C.D. "An Electron Fractographic Study of the Influence of Plastic Strain Conditions Upon Ductile Rupture Processes in Metals", trans. of the ASM, 5b, 318-326, (1963).
2. Rogers, H.C., "The Tensile Fracture of Ductile Metals", Trans. of the Metallurgical Society of AIM, 218, 498-506, (1960).

3. Weinrich, P.E. and Frensh, I.E., "The Influence of Hydrostatic Pressure on the Fracture Mechanisms of Sheet Tensile Specimens of Copper and Brass", *Acta Met.*, 24, 317-322, (1976)
4. Beevers C.J. and Honey Combe R.W.K., *Phil. Mag.*, 7, 763-773, (1973).
5. Baver R.W. and Wilsdorf H.G.F., *Acta Met.*, 23, 269-277, (1975).
6. Lyles R.L. and Wilsdorf H.G.F., *Acta Met.* 24, 317-322, (1976).
7. Fat-halla, N., Takasugi, T. and Izumi, O., "Dynamic Observations of the Fracture Phenomena in  $\alpha/\beta$  Brass Two-Phase Bicrystals", *J. of Mat. Science*, 13, 2462-2470, (1978).
8. Takasugi, T., Fat-halla, N. and Izumi, O., "The Plastic Deformation and Fracture Behaviours of  $\alpha - \beta$  Brass Two-Phase Bicrystals", *Acta Met.*, 26, 1453-1459, (1978).
9. Takasugi, T., Fat-halla, N., and Izumi, O., "Deformation and Fracture of  $\alpha - \beta$  -Brass-Two-Phase Bicrystals".
10. Fat-halla, N., Takasugi, T., and Izumi, O., "Deformation and Fracture of  $\alpha - \beta$  Brass Two-Phase Bicrystals at 450 K" *Trans. JLM*, 20, 493-500, (1979).
11. Fat-halla, N., Takasugi, T., and Izumi, O., "Deformation and Fracture of  $\alpha - \beta$  Brass Two-Phase Bicrystals at 150 K" *Metal. Trans. A*, 10A, 1341-1349, (1979).
12. Takasugi, T., Izumi, O., and Fat-halla, N., "Transgranular Slip and Fracture Across an Interface in  $\alpha/\beta$  Brass Two-Phase Bicrystals" *J. of Mat. Science*, 15, 945-950, (1980).
13. French, I.E., Weinrich, P.F. and Weaver, C.W., "Tensile Fracture of Free Machining Brass as a Function of Hydrostatic Pressure", *Acta Met.*, 21, 1048-1049, (1973).
14. French, I.E. and Weinrich, P.F., "The unusual variation of the Tensile Fracture Strain of Brasses at High Pressures", *Scripta Metallurgica*, 8, 7-10, (1974).
15. French, I.E. and Weinrich, P.E., "The Shear Mode of Ductile Fracture in Materials with Few Inclusions", *Acta Met.*, 24, 317-322, (1976).
16. Przystupa, M.A., Stout, M.G. and Courtney, T.H., "The Interaction Between Deformation, Fracture Initiation, and Fracture Propagation in Two Phase", *Met. Trans.*, 11A, 643-651, (1980).
17. Przystupa, M.A. and Courtney, T.H., "Fracture in Alloys with Isolated Elastic Particles", *Met. Trans.*, 13A, 873-859, (1982).
18. Davis, R.J., Pearee R., and Rothery W.H., *Acta Cryst.*, 5-36, (1952).
19. *Metals Handbook (ASTM) Fractography and Atlas of Fracture*, (1974).
20. John R. Low, Jr., "Progress in Materials Science. The Fracture of Metals", B. Chalmers, 12, Pergamon Press Oxford London New York, (1965).

